

Effect of growth restricting factor on grain refinement of aluminum alloys

T. Chandrashekar · M. K. Muralidhara ·
K. T. Kashyap · P. Raghothama Rao

Received: 2 December 2006 / Accepted: 30 November 2007 / Published online: 9 January 2008
© Springer-Verlag London Limited 2007

Abstract Grain structure is an important and readily observable feature in aluminum alloy castings. Depending on the constitutional and heat-flow conditions in a solidified aluminum alloy, various morphologies are possible. Grain refining is one of the predominant techniques in controlling the quality of castings. It plays a vital role in improving metallurgical characteristics and mechanical properties of aluminum alloys. Fine equiaxed grains ensure remarkable benefits. There are a number of techniques to achieve fine equiaxed grain structure, but grain refinement by the addition of grain refiners referred to as inoculation is the most popular due to its simplicity. Grain refinement has been studied extensively by researchers for several decades, not only for developing efficient grain refiners but also for achieving an understanding of the mechanism of grain refinement. In spite of its commercial importance, benefits and numerous

scientific studies in this area, the grain refinement of aluminum and its alloys is still a controversial subject. Solute elements like titanium segregate to the inoculants/melt interface affecting the dendrites and also affect the constitutional undercooling at the solid–liquid interface. This segregating power of an element is quantified by the growth restricting factor (GRF). In the present investigation, the effect of GRF on grain refinement of aluminum-silicon alloys was studied by the addition of Al-5Ti-1B master alloy. It is evident from this investigation that the growth rate of grains is inversely proportional to the GRF.

Keywords Grain refinement · Undercooling · Alcan test · $TiAl_3$ phase · Growth restricting factor (GRF)

T. Chandrashekar (✉)
Department of Mechanical Engineering,
Sri Venkateshwara College of Engineering,
Vidyanagar, Near Yelahanka Airforce, Bettahalasuru,
Bangalore 562 157, India
e-mail: chandrashekarthi@yahoo.com

M. K. Muralidhara
Department of Mechanical Engineering,
M.S. Ramaiah Institute of Technology,
Bangalore, India

K. T. Kashyap
Department of Mechanical Engineering,
PES Institute of Technology,
Bangalore, India

P. R. Rao
Center for Military Airworthiness and Certification,
Defence Research and Development Organization,
Ministry of Defence, Government of India,
Bangalore, India

1 Introduction

Grain refinement of aluminum alloys is an important area of study and has advantages in various applications. Grain structure is an important and readily observable feature in aluminum alloy castings. Depending on the constitutional and heat-flow conditions in a solidified aluminum alloy, three different grain morphologies are possible [2]: equiaxed, columnar, and twinned columnar grains (TCG). Grain refining is one of the predominant techniques for controlling the quality of castings. It may be defined as the deliberate suppression of columnar and twinned columnar grains and to favor fine equiaxed grains by the addition of grain refiners to the molten metal before pouring. Grain refinement plays a vital role in improving metallurgical characteristics and mechanical properties of aluminum alloys. Fine equiaxed grains ensure the following benefits: (i) uniform and improved mechanical properties throughout the material, (ii) distribution of secondary phases and micro-porosity on a

fine scale which in turn improves machinability, (iii) better feeding to eliminate shrinkage porosity, (iv) improved ability to achieve uniformly anodized surface and super plasticity, (v) better surface finishes on both the basic casting and the machined parts (cosmetic features), (vi) reduced ingot cracking and improved resistance to hot tearing, (vii) better strength, toughness, fatigue life and corrosion resistance.

2 Literature review

2.1 Mechanism of grain refinement

In principle, the mechanism of grain refinement appears to be very simple [2]. First, numerous potent heterogeneous nucleating sites must be introduced into the melt and second, constitutional heat and fluid flow conditions must be such that a large number of these sites actually become active and nucleate solid. In other words, the growth of the nucleated grains must not be too rapid otherwise those which form first will grow quickly and consume nucleation sites, which will reduce the number of nuclei capable for further growth. It is, however, much more difficult to explain fully how Al-Ti and Al-Ti-B grain refiners operate as evidenced by the volume of work on the topic over the years. It is agreed that when refiners are added to Al-alloy melts, the aluminum matrix dissolves and releases intermetallic particles into the melt. However, exactly which particles are released, their physical and chemical character, and their subsequent reaction with the melt are still disputed. Several mechanisms have been postulated [9], but no clear consensus has emerged as yet.

2.2 Grain refinement theories

One of the first extensive grain-refining studies was presented by Cibula [1] and was followed by F.A. Crossley and L.F. Mondolfo [3]. Later, various theories have been put forth by the research workers on the mechanism of the grain refinement. Mark Easton and David St. John [9] reviewed all the theories and classified them as nucleant paradigm and solute paradigm. The nucleant paradigm deals with the heterogeneous nucleation of solid aluminum on some nucleating sites, while the solute paradigm incorporates the influence of solute elements on the grain-refinement process.

2.2.1 Nucleant paradigm

Grain refinement can be understood to be directly related to the nucleation and growth process of aluminum grains. This is based on the nucleation ideas of Volmer and Weber [13]. The theory involves homogeneous and heterogeneous

nucleation. The critical nucleus size for survival in a pure solidifying metal is given by

$$r_{homogeneous}^* = \frac{-2\gamma_{sl}}{\Delta G_v} \tag{1}$$

The free energy barrier is given by

$$\Delta G_{homogeneous}^* = \frac{16\pi\gamma_{sl}^3}{3\Delta G_v^2} \tag{2}$$

Where, γ_{sl} is the interface surface energy of a solid-liquid interface in J/m², assuming the specific heats of liquid and solid are similar. ΔG_v is the driving force for solidification and is

$$\cong \Delta T \Delta S = \frac{\Delta H_f \Delta T}{T_m}$$

ΔT is the undercooling below the liquidus temperature K, ΔS the entropy change for liquid to solid phase transformation J/K/m³, ΔH_f the enthalpy of solidification and T_m the melting temperature. If the embryo of the solid is greater than the critical radius, $r_{homogeneous}^*$, the embryo will survive and become a nucleus.

In heterogeneous nucleation, the critical nucleus size is

$$r_{heterogeneous}^* = \frac{-2\gamma_{sl}}{\Delta G_v} \tag{3}$$

Equations (1) and (3) are identical for both homogeneous and heterogeneous nucleation and the free energy barrier is

$$\Delta G_{heterogeneous}^* = \frac{16\pi\gamma_{sl}^3}{3\Delta G_v^2} f(\theta) \tag{4}$$

Where $f(\theta)$ is a function of the contact angle, θ on the substrate on which nucleation takes place. Figure 1 shows the solid nucleating on a substrate in a liquid. Figure 2 shows the variation of $f(\theta)$ with θ and since $f(\theta)$ is always ≤ 1 , the critical free energy for heterogeneous nucleation is always less than or equal to that for homogeneous nucleation. However, it is clear that potent heterogeneous substrates are those with θ close to zero.

The values of undercooling, ΔT is of the order 1–2 K for observable nucleation rates in commercial aluminum alloys with grain refiners. Therefore, clearly heterogeneous nucle-

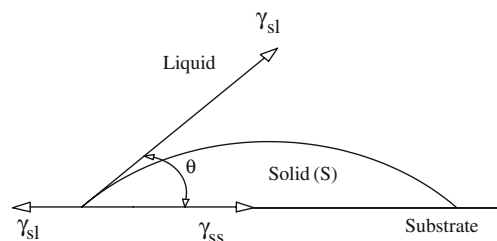


Fig. 1 Schematic representation showing the formation of spherical cap of solid(s) on a substrate, contact angle and surface tension forces [2]

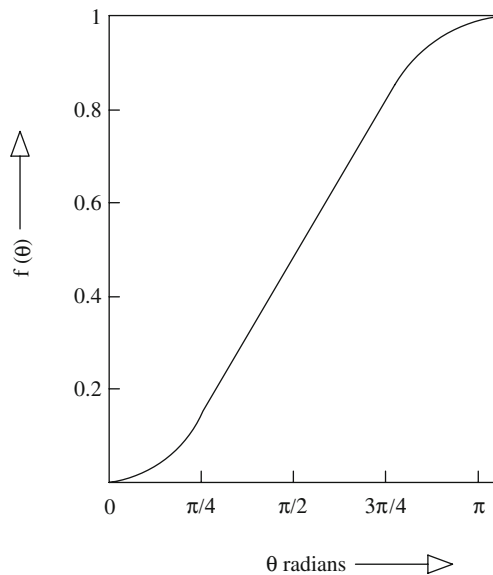


Fig. 2 Variation of $f(\theta)$ with θ where $f(\theta)$ is equal to $(2 - 3 \cos \theta + \cos^3 \theta)/4$ [2]

ation is taking place. The following simplified expression for heterogeneous nucleation rate per unit volume in $\text{m}^{-3} \text{s}^{-1}$ is

$$I_{\text{heterogeneous}}^v = 10^{18} N_v^p \exp \left[\frac{-16\pi\gamma_{sl}^3 f(\theta)}{3K_B \Delta S^2 \Delta T^2} \right] \quad (5)$$

Where, K_B is the Boltzmann's constant, J/K, N_v^p the number of nuclei/ m^3 , and $I_{\text{heterogeneous}}^v$ the heterogeneous nucleation rate of nuclei / $\text{m}^3 \text{s}$.

Therefore, it can be seen that if the contact angle is close to zero, wetting of the substrate for nucleation is promoted and the nucleation rate increases.

Growth of nuclei Once nucleation takes place, more importantly heterogeneous nucleation, the growth front of the nuclei is seldom planar. The well-known constitutional

supercooling occurs as solute is rejected at the interface and the criterion is given by [7].

$$\frac{G_L}{R} \geq \frac{-m_L C_0 (1 - k)}{k D_L} \quad (6)$$

where, G_L is the temperature gradient in the liquid ahead of the solid–liquid interface (K/m). R the growth rate of phase diagram (K/wt%), C_0 the bulk alloy composition in the liquid (wt%), k the partition coefficient between solid and liquid, and D_L the diffusion coefficient of the solute in the liquid (m^2/s).

Normally, in a casting we have a columnar zone and a central portion of equiaxed crystals [4]. The columnar dendrites grow in [100] directions in the cubic system and growth direction is antiparallel to the heat flow direction. The equiaxed dendrites grow in the same direction of heat flow, i.e., radially outward. The formation of equiaxed crystals is due to dendrite arm melt off [5], which provides nuclei for equiaxed crystals.

2.2.2 Solute paradigm

This theory was proposed by Mats Johansson et al. [10] and suggests that the nucleation occurs on borides or other particles. According to this theory, additions of both the nucleant particles and the amount of segregating elements, quantified by the growth restriction factor (GRF) are important in grain refinement. It was found that there is a low discrepancy of 4.3% between $\alpha\text{-Al}$ and TiB_2 , indicating TiB_2 as a good nucleant. The solutes affect the dendrite growth and builds up a constitutionally undercooled zone in front of the interface. This undercooled zone facilitates

Table 1 Segregating power of some elements in aluminum [9]

Element	k_i	m_i	$(k-1)m$	Max. concentration (Wt.%)	Reaction type
Ti	~9.0	30.7	245.6	0.15	Peritectic
Ta	2.5	70.0	105.0	0.10	Peritectic
V	4.0	10.0	30.0	~0.1	Peritectic
Hf	2.4	8.0	11.2	~0.5	Peritectic
Mo	2.5	5.0	7.5	~0.1	Peritectic
Zr	2.5	4.5	6.8	0.11	Peritectic
Nb	1.5	13.3	6.6	~0.15	Peritectic
Si	0.11	-6.6	5.9	~12.6	Eutectic
Cr	2.0	-3.5	3.5	~0.4	Peritectic
Ni	0.007	-3.3	3.3	~6.0	Eutectic
Mg	0.51	-6.2	3.0	~3.4	Eutectic
Fe	0.02	-3.0	2.9	~1.8	Eutectic
Cu	0.17	-3.4	2.8	33.2	Eutectic
Mn	0.94	-1.6	0.1	1.9	Eutectic

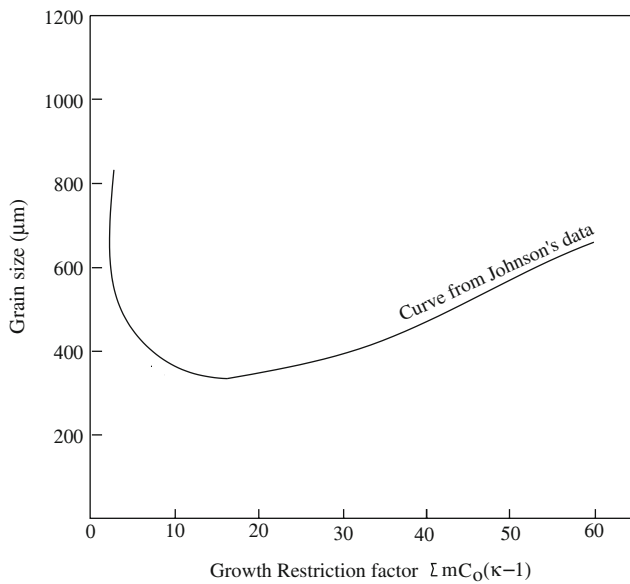


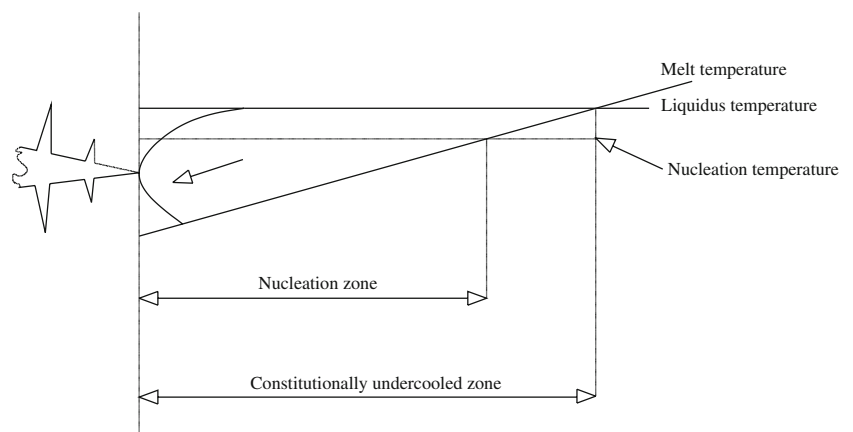
Fig. 3 Graph of grain size data plotted against the growth restricting factor (GRF) [9]

nucleation and the new grains do the same to the next grain. Solute elements like titanium segregate to the inoculant/melt interface and affect the growth of dendrites and also affect the constitutional undercooling at the solid–liquid interface.

During solidification, the segregating power of an element is described by growth restricting factor (GRF), which is a measure of the growth-restricting effect of solute elements on the growth of solid–liquid interface of the new grains as they grow into the melt. The GRF may be defined as $mC_0(k-1)$, where m is the liquidus gradient, C_0 the bulk composition, k the partition coefficient between solid and liquid. Typical values of these parameters for common alloying elements are presented in Table 1.

When a number of solutes are present in the melt, the GRF's are added, which assumes that there is no interaction between solutes. GRF for an alloy is $\sum m_i C_0 (k_i - 1)$.

Fig. 4 Diagram showing constitutionally undercooled region in front of growing dendrite and the zone in which nucleation can occur, if nucleant particles are present. The size of this zone will change depending on the potency of the nucleant and the constitution of the melt. If Ti is present the size of the undercooled zone will increase [9]



The criterion for constitutional supercooling is

$$\frac{G_L}{R} \geq \frac{-\sum m_i C_0 (1 - k_i)}{k D_L}$$

We can see that the growth rate is inversely proportional to $\sum m_i C_0 (k_i - 1)$. Li et al. [8] have suggested that the reason for grain refinement caused by titanium additions is due to the titanium as a solute. They suggest that the powerful segregating ability of titanium as a solute leads to a constitutional undercooled zone in front of the growing interface within which nucleation can occur on nucleants that are present. Cast alloys are more difficult to grain refine than wrought alloys. The reason for this is thought to be the high level of alloying elements particularly silicon.

Relationship between solute and dendrite growth The solute effect of Ti, Si, and Fe has been studied by Johnson and Backerud [6] who found that these elements restricted the growth rate of dendrites and are additive in effect which is quantified by GRF. Spittle and Sadli [11] performed similar experiments with Al-5Ti-B on a wide range of solute elements and found that the grain size dropped dramatically with increase in GRF. Figure 3 shows a graph of grain size versus GRF from Spittle and Sadli's work which shows that an initial rapid decrease in grain size with GRF is seen and further addition of solute produces no effect but after a GRF value of 20, the grain size began to increase.

The solute effects of Si produces grain refinement at about 3 wt%, while Ti only needs to be added at concentration of about 0.1 wt% for optimum grain-refining effectiveness. These are equivalent GRF's (i.e., 17.7 for 3 wt% Si and 24.5 for 0.1 % Ti).

According to Johnson and Backerud [6], the grain size begins to increase once again above a critical value due to a change in the growth mechanism of dendrites. At low GRFs, solute slows down growth of the dendrite, due to diffusion of solute in front of the interface. But at higher

concentrations, the dendrites develop lancet-like tips that grow into the liquid and reject solute orthogonally to the growth direction. This is due to the change from diffusion controlled growth, to dendrite tip radius controlled growth, where capillary effects dominate.

In the recent work of Spittle et al. [12] in Al-Zn system, there was no increase of grain size after the minimum, as more solute was added. Solute was added up to a GRF of 50. This is very different from Johnsson's (1996) Al-Si alloys. Therefore solute effect depends on the system also. Thus further research is needed to understand the solute effects particularly interaction between solutes and their effect on GRF.

Recently, Easton and St. John [9] have shown that in Al-2Si and Al-0.05%Ti, addition of TiB₂ particles refines the grain size to the same extent. Both Al-2Si and Al-0.05%Ti have the same GRF. Further, they have also shown that the measured partition coefficient 'k' for Ti is 6.7 compared with phase diagram prediction of 7.5 in pure Al and 3.2 for Ti in Al-7Si-0.3 Mg alloy. The low partition coefficient of Ti in Al-Si alloys is seen to be responsible for the poor grain refining effectiveness of Ti. The partition coefficient of Ti in pure Al is 7.5 whereas it is only 3.2 in Al-7Si-0.3 Mg alloy. The GRF given by $mC_0(k-1)$, which would be large in Al and low in Al-7Si-0.3 Mg alloy. Therefore, the constitutional undercooling in high purity Al would be larger when compared to Al-7Si-0.3 Mg cast alloy. Therefore, the solute effect of Ti would be greater in high purity Al than in Al-7Si-0.3 Mg alloy. To summarize, the solute effect is shown in Fig. 4 where the constitutional undercooling zone is shown in front of a growing dendrite tip. If the GRF for a solute is large, this undercooled zone will be large. If nucleant particles are present in sufficient number (like AlB₂, TiB₂ etc), these particles nucleate α -Al in the supercooled zone. This process repeats itself leading to a very fine grain size.

In the light of the above literature, it may be proposed that the constitutional undercooling ahead of the solid-liquid interface activates nuclei ahead of the interface. Therefore in the present investigation the effect of GRF on grain refinement of Al alloys was studied by the addition of Al-5Ti-1B master alloy.

3 Experimentation

Initially, the Al-5Ti-1B master alloy was characterized completely by JEOL-840 SEM and transmission electron microscopy (TEM) by PHILLIPS Em 430T. For TEM, the samples were electro polished with 30% nitric acid in methanol solution, at 30°C using 12 V dc, and observed under 250 kV two beam condition. Then, four Al alloys

namely; LM24, LM9, LM25 and LM6 were selected which possess different values of GRF. These four alloys were further subjected to spectroscopy for chemical analysis. The chemical composition obtained by spectroscopic analysis and the corresponding GRF's were calculated as shown in the Table 2.

Each of the above-mentioned four alloys were melted individually and stabilized at 720°C in a resistance furnace. The characterized Al-5Ti-1B master alloy was then added

Table 2 Results of spectroscopic chemical analysis and their calculated GRF's

Alloying elements	Composition in wt%	Segregating power $m(k-1)$	GRF $mC_0(k-1)$
Alloy: LM24			
Si	8.118	5.9	47.896
Fe	1.135	2.9	3.292
Cu	3.026	2.8	8.473
Mn	0.251	0.1	0.025
Mg	0.268	3.0	0.804
Ni	0.092	3.3	0.304
Zn	1.181	–	–
Pb	0.263	–	–
Total of GRF or $\sum mC_0(k-1)$			60.794
Alloy: LM9			
Si	10.129	5.9	59.761
Fe	0.437	2.9	1.2673
Cu	0.054	2.8	0.1512
Mn	0.374	0.1	0.0374
Mg	0.390	3.0	1.1700
Ni	0.007	3.3	0.0231
Zn	0.061	–	–
Pb	0.003	–	–
Total of GRF or $\sum mC_0(k-1)$			62.410
Alloy: LM25			
Si	6.85	5.9	38.822
Fe	0.29	2.9	0.841
Cu	0.052	2.8	0.1456
Mn	0.039	0.1	0.0039
Mg	0.45	3.0	1.35
Ni	0.004	3.3	0.0132
Ti	0.126	246.55	31.065
Al	Remaining	–	–
Total of GRF or $\sum mC_0(k-1)$			72.2407
Alloy: LM6			
Si	12.994	5.9	76.6646
Fe	0.55	2.9	1.595
Cu	0.24	2.8	0.672
Mn	0.087	0.1	0.0087
Mg	0.251	3.0	0.753
Ni	0.02	3.3	0.066
Ti	0.029	246.55	7.1224
Al	Remaining	–	–
Total of GRF or $\sum mC_0(k-1)$			86.8817

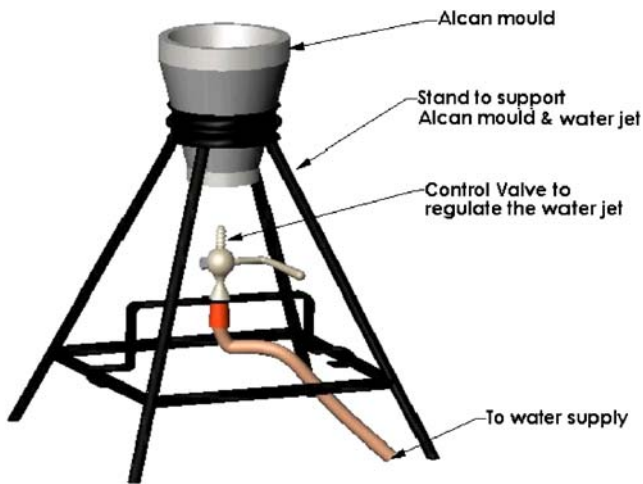


Fig. 5 A model showing complete details of Alcan experimental set up

to these alloys to attain an addition level of 0.05%Ti in the melt. The melt samples were cast by using the standard Alcan experimental setup as shown in Fig. 5, at every 10 min for a holding period of up to 60 min to study the fading effect of the grain refiner in the melt. Finally, the grain sizes were measured by standard metallographic methods.

4 Results and discussion

Figure 6 shows the SEM image of the Al-5Ti-1B master alloy used in the present investigation to grain refine the four Al alloy systems. It is very clear that the particles present in the master alloy are blocky in nature.

The EDAX pattern of these particles (Fig. 7) showed only Al and Ti peaks indicating the presence of only TiAl₃

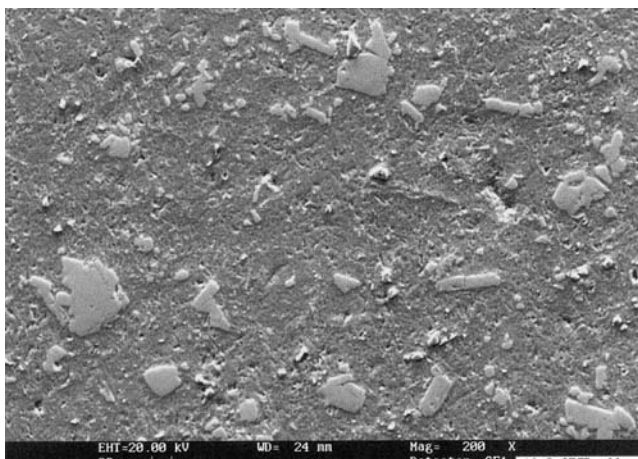


Fig. 6 SEM photograph of Al-5Ti-1B master alloy showing blocky particles

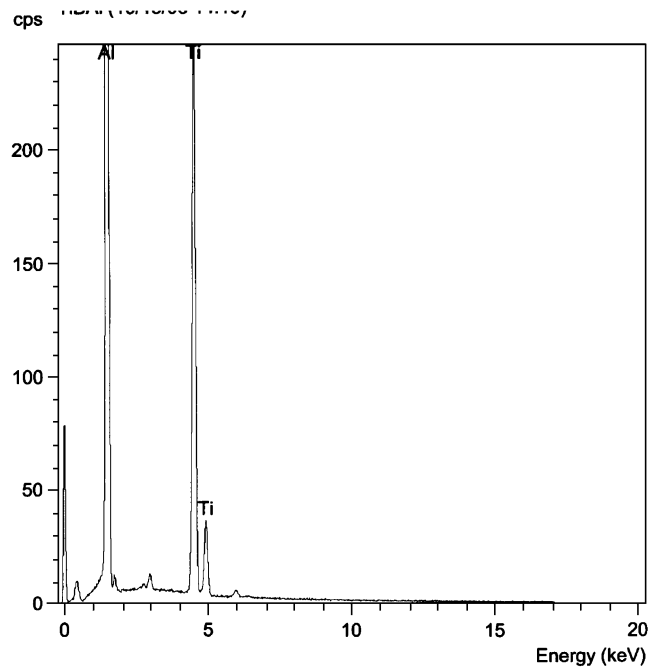


Fig. 7 EDAX spectrum indicating only Al & Ti peaks confirming blocky crystals are TiAl₃

phase, and since no B peaks were observed, which confirms the absence of either TiB₂ or AlB₂ phases.

The bright field image (TEM) and the associated selected area diffraction pattern (SAD) were as shown in Fig. 8a and b, respectively. While Fig. 9 shows a schematic analysis of the above SAD pattern. Indexing of this SAD pattern confirmed that the blocky particles were FCC metastable L1₂ structure of TiAl₃. The lattice parameter of this phase was found to be 4Å⁰, and the discrepancy between Al and TiAl₃ was found to be only 0.9%, which, clearly indicates that this phase actually nucleates α-Al. Further, this phase was consistent with the metastable TiAl₃ phase observed by W.T. Kim et al. [14].

The average grain sizes of the above mentioned (i.e., LM24, LM9, LM25 and LM6) alloys refined by Al-5Ti-1B

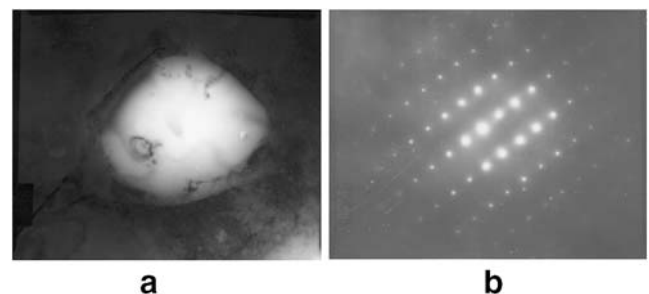


Fig. 8 a Bright field image (TEM) of TiAl₃ particle in an Al-5Ti-1B master alloy. b Corresponding SAD pattern from the TiAl₃ particle

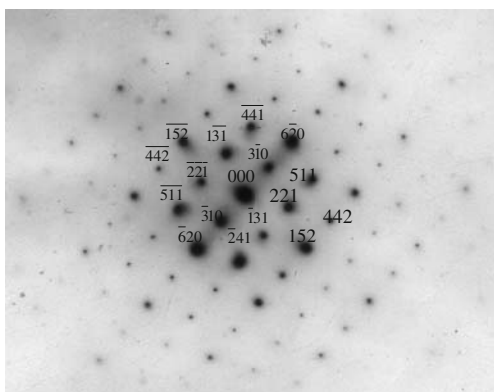


Fig. 9 Schematic analysis of the SAD pattern for the $TiAl_3$ particle in Al-5Ti-1B master alloy

master alloy at an addition level of 0.05%Ti with respect to holding time of up to 60 min are shown in Fig. 10.

It can be seen that the average grain sizes were reduced considerably in each of the alloy systems upon the addition of Al-5Ti-1B master alloy. It can be observed that there is no fading effect of Al-5Ti-1B master alloy in the above alloy systems even up to a holding period of 60 min. Further, it is evident that the average grain sizes calculated over a period of 60 min are 1,681, 1,318, 942 and 460 μm for LM24, LM9, LM25 and LM6 alloy systems, respec-

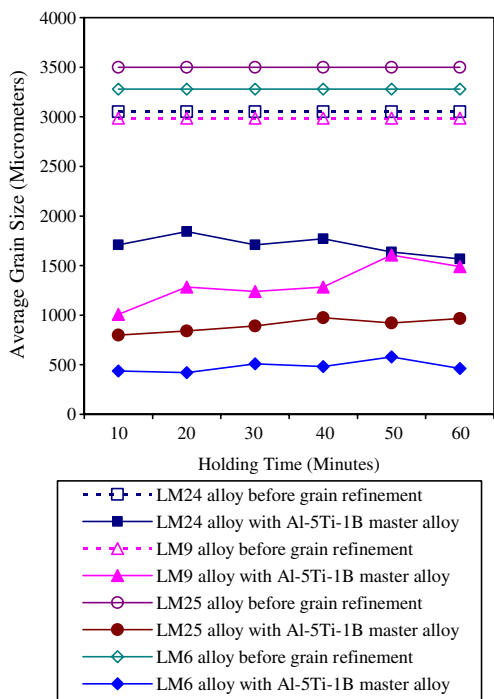


Fig. 10 Graph showing average grain sizes versus holding time for LM24, LM9, LM25 and LM6 alloys grain refined by Al-5Ti-1B master alloy

tively. It is also evident from Table 2 that the calculated values of GRF are 60.794, 62.410, 72.2407, and 86.8817, respectively, for LM24, LM9, LM25 and LM6 alloy systems. Thus, it can be concluded that the extent of grain refinement achieved upon the addition of Al-5Ti-1B master alloy may be directly attributed to the GRF's of the corresponding alloy system.

Figure 11 shows the extent of grain refinement with respect to the GRF for the four alloy systems which are grain refined by Al-5Ti-1B master alloy. From this it is very clear that as the GRF of an alloy system increases there will be a corresponding decrease in the grain size.

This result is in support of the solute paradigm proposed by Mark Easton and David St. John [9]. This implies that although the borides are absent in the master alloys, the metastable $L_{12} - TiAl_3$ phase nucleates α Al provided growth restricting conditions for dendrites are present in the system. Consistent with Johnson et al. (1993), no matter what the nucleating particle is (i.e., as long as nucleating conditions are favourable, i.e., low disregistry and so on), the solute effects (GRF) control the final grain sizes of the alloy system.

5 Conclusions

Addition of Al-5Ti-1B master alloy results in a significant grain refinement of LM24, LM9, LM25 and LM6 alloy systems. It is evident that grain refinement of Al alloys is by heterogeneous nucleation and growth of grains. It is also apparent that the nucleating effects in grain refinement are important but the solute effects play a vital role. The segregating power of Ti is very high and it segregates to the nucleant-liquid interface, which leads to constitutional supercooling within which other nucleant particles get activated for nucleation. Finally, it can be concluded that the growth rate is inversely proportional to the GRF.

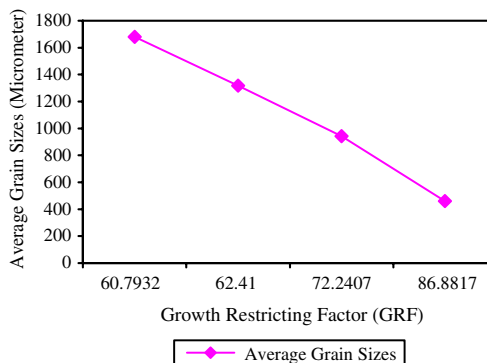


Fig. 11 Average grain sizes versus the growth restricting factor (GRF) for various aluminum alloy systems

Acknowledgements Authors are thankful to: M.S. Ramaiah Institute of Technology, Bangalore. University Visvesvaraya College of Engineering, Bangalore University, Bangalore. Hindustan Aeronautics Limited, Foundry & Forge Division, Bangalore. Defence Metallurgical & Research Laboratory, Hyderabad, for extending their help in carrying out the present investigation.

References

1. Cibula A (1949–50) Grain refinement of aluminium alloy by TiC. *J Inst Metals* 76:321–360
2. McCartney DG (1989) Grain refining of aluminium and its alloys using inoculants. *Int Mater Rev* 34(5):247–260
3. Crossley FA, Mondolfo LF (1951) Mechanism of grain refinement in aluminium alloys. *Trans AIME* 191:1143–1151, (December 1951)
4. Flemings MC (1974a) Solidification processing. In: Stephen M et al (eds) McGraw-Hill Inc., USA, Chap. 5, p 135
5. Flemings MC (1974b) Solidification processing. In: Stephen M et al (eds) McGraw-Hill Inc., USA, Chap. 5, p 151
6. Johnsson M, Backerud L (1996) *Z Meta Kd* 87:216
7. Kurz W, Fisher DJ (1984) Fundamentals of solidification. *Trans. Tech. Publications, Switzerland*, p 47
8. Li H, Sritharan T, Lam YM, Leng NY (1997) *J Mater Sci Technol* 66:253
9. Easton M, St. John D (1999) Grain refinement of aluminium alloys: Part I. The nucleant and solute paradigms - a review of the literature. *Metall Mater Trans* 30A:1613–1623, (June 1999)
10. Johnsson M, Backerud L, Sigworth GK (1993) Study of the mechanism of grain refinement of aluminium after additions of Ti - and B - containing master alloys. *Metall Trans* 24A:481–491, February
11. Spittle JA, Sadli S (1995) *Mater Sci Technol* 11:533–537
12. Spittle JA, Keeble JM, AlMeshedani M (1997) Light metals. In: Huglen R (ed) TMS, Warrendale, PA, p 795
13. Volmer M, Weber A (1925) *Z Krift Phys Chem* 119:277
14. Kim WT, Cantor B, Griffith WD, Jolly MR (1992) *Int J Rapid Solidif* 7:245–254